Journal of Computer Science & Computational Mathematics, Volume 5, Issue 1, March 2015
DOI: 10.20967/jcscm.2015.01.001

Stagnation Point Flow over a Permeable Shrinking Sheet with Slip Effects: Suction Case

Nur Fatihah Fauzi[1*], Syakila Ahmad[1], Lok Yian Yian[2], Ioan Pop[3]

[1] School of Mathematical Sciences, Universiti Sains Malaysia, 11800 USM, Penang, Malaysia,
[2] Mathematics Section, School of Distance Education, Universiti Sains Malaysia, 11800 USM, Penang, Malaysia,
[3]Department of Mathematics, Babeș-Bolyai University, 400084 Cluj-Napoca, Romania,
[*]Corresponding author email: nurfatihah.fauzi@gmail.com

Abstract: In this study, a steady stagnation point flow due to a permeable shrinking sheet with the slip effects is investigated. Employing similarity transformations, the governing boundary layer equations are transformed into the nonlinear ordinary differential equations. The transformed equations are figured out numerically using the shooting method. Results show that dual solutions for velocity and temperature distribution exist for a certain range of the shrinking parameter. The results also indicate that the skin friction coefficient and the local Nusselt number increase for the upper branch solution as the suction parameter increases. Meanwhile, for the lower branch solution, the skin friction coefficient decreases and the local Nusselt number increases as the suction parameter increases. It is also found that the velocity slip and suction process delay the boundary layer separation whereas the temperature slip does not affect the boundary layer separation.

Keywords: boundary layer, stagnation point flow, shrinking sheet, slip effects, dual solutions.

1. Introduction

The boundary layer flow due to shrinking sheets is very significant for many practical applications in advanced manufacturing. It seems that the steady two-dimensional stagnation-point flow towards a stretching sheet was first investigated by Chiam [1] considering the strain-rate of the stagnation-point flow and the stretching rate of the sheet to be equal. Mahapatra and Gupta [2,3] studied the same problem considering the strain-rate and the stretching rate to be different. Weidman et al. [4] have pictured the forced convection boundary layer flow past a semi-infinite plate that concentrates the simultaneous effects of transpiration and plate movement. Presently, the slip effects towards a stretching or shrinking sheet have been the field of many studies among researchers. Wang [5] investigated the flow of a stretching flat boundary due to partial slip which is solved by similarity transformation. Rosca and Pop [6] developed a mathematical model to study the flow and heat transfer over a vertical permeable stretching/shrinking sheet using a second order slip flow model. They reported that the second order slip flow model is requisite to anticipate the flow characteristics accurately. Aman et al. [7] numerically solved the hydromagnetic stagnation point flow towards a stretching/shrinking sheet with slip effects on the boundary. They described the effect of magnetic, slip and stretching/shrinking on skin friction and heat transfer rate. Furthermore, the behavior of flow and heat transfer over a vertical shrinking sheet with suction was discussed by Rohni et al. [8,9] involving exponential velocity and temperature distribution. Suction or injection of a fluid through the bounding surface, for example, in mass transfer cooling, can significantly change the flow field and, as a consequence, can affect the heat transfer rate at the plate. In general, suction tends to increase the skin friction and heat transfer coefficients, whereas injection acts in the opposite manner (Al-Sanea [10]). Injection or withdrawal of a fluid through a porous bounding heated or cooled wall is of general interest in practical problems involving boundary layer control applications such as film cooling, polymer fiber coating, coating of wires, etc. The stretching/shrinking sheets are relevant to many manufacturing industries, such as, paper production, polymer processing, glass-fiber production, etc. (Sparrow and Abraham [11]). It appears that flow towards a shrinking sheet was widened by Bhattacharyya [12], Bhattacharyya et al. [13], Bhattacharyya and Pop [14], Bhattacharyya and Layek [15] and Bhattacharyya and Vajravelu [16]. In the meantime, Vajravelu [17], Nazar et al. [18], Nadeem et al. [19] and Rohni et al. [20] have explored the flow and heat transfer over a stretching sheet under different physical aspects by using the fourth-order Runge-Kutta integration scheme, the Keller-box method and the homotopy analysis method (HAM). Further, Bhattacharyya [21] and Yao et al. [22] have contemplated the problem for both shrinking and stretching sheets and walls, respectively, with time dependent surface temperature and convective boundary conditions. There are also several important published papers on this topic, such as Seini et al. [23], Makinde [24], Shateyi and Makinde [25], Makinde et al. [26], Olanrewaju and Makinde [27], Roşca and Pop [28], and Roşca et al. [29].

Motivated by the work reported by Weidman et al. [4] and Bhattacharyya et al. [13], we extended the problem by investigating the steady stagnation point flow over a permeable shrinking sheet with velocity and temperature slip effects. To the authors' present knowledge, this study has not been reported in literature and it is hoped that the results will serve as a complement to the previous studies as well as to provide useful information for real applications.

2. Basic Equations

Consider a steady, two-dimensional laminar flow and heat transfer of a viscous and incompressible fluid near the stagnation point past a permeable shrinking surface coinciding with the plane $y=0$ where the fluid occupies the upper half plane $(y \geq 0)$ as it is shown in Figure 1. Here y is the coordinate measured normal to the surface of the sheet in a vertical direction and the x coordinate is measured along the surface of the shrinking sheet. It is assumed that the shrinking surface has a variable velocity $u_w(x)$ and a variable temperature $T_w(x)$, while the velocity of the flow external to the boundary layer is $u_e(x)$ and the temperature is T_∞. It is also assumed that the mass flux velocity is $v_w(x)$, where $v_w(x)<0$ corresponds to suction and $v_w(x)>0$ corresponds to injection. Under these assumptions, the governing boundary layer equations are given as (Bhattacharyya et al. [13]):

$$\frac{\partial u}{\partial x}+\frac{\partial v}{\partial y}=0 \tag{1}$$

$$u\frac{\partial u}{\partial x}+v\frac{\partial u}{\partial y}=u_e(x)\frac{d u_e(x)}{d x}+\nu\frac{\partial^2 u}{\partial y^2} \tag{2}$$

$$u\frac{\partial T}{\partial x}+v\frac{\partial T}{\partial y}=\alpha\frac{\partial^2 T}{\partial y^2} \tag{3}$$

with boundary conditions of:

$$\begin{aligned} &v=v_w(x), \quad u=u_w(x)+M(x)\mu\frac{\partial u}{\partial y} \\ &T=T_w(x)+N(x)\mu\frac{\partial T}{\partial y} \quad \text{at} \quad y=0 \\ &u\to u_e(x), \quad T\to T_\infty \quad \text{as} \quad y\to\infty \end{aligned} \tag{4}$$

where u and v are the velocity components along x and y axes, respectively, T is the temperature, α is the thermal diffusivity of the fluid, μ is the dynamic viscosity, ν is the kinematic viscosity, ρ is the density, $M(x)$ and $N(x)$ are the velocity and temperature slip variables, respectively, and λ is the constant stretching $(\lambda>0)$ or shrinking $(\lambda<0)$ parameter. We assume here that $u_w(x)$, $u_e(x)$, $T_w(x)$, $M(x)$ and $N(x)$ have the following forms:

$$\begin{aligned} &u_w(x)=c\,x^m, \quad u_e(x)=a\,x^m(x), \quad T_w(x)=T_\infty+T_0\,x^n \\ &M(x)=\sqrt{2/a\nu(m+1)}\,x^{(1-m)/2}\,A/\rho \\ &N(x)=\sqrt{2/a\nu(m+1)}\,x^{(1-m)/2}\,B/\rho \end{aligned} \tag{5}$$

where a, m, n and T_0 are positive constants, while $A(>0)$ and $B(>0)$ are constant slip parameters, and the constant $c>0$ corresponds to a stretching and $c<0$ corresponds to a shrinking sheet. Further, it is worth mentioning that $m=1$ corresponds to the stagnation point flow, $n=0$ corresponds to the constant surface temperature and $n=1$ corresponds to the linearly variation of the surface temperature, respectively.

We introduce now the following similarity variables

$$\begin{aligned} &\psi=\sqrt{\frac{2\nu a}{m+1}}\,x^{\frac{m+1}{2}}\,f(\eta), \quad \theta(\eta)=\frac{T-T_\infty}{T_w-T_\infty} \\ &\eta=y\,x^{\frac{m-1}{2}}\sqrt{\frac{a(m+1)}{2\nu}} \end{aligned} \tag{6}$$

where ψ is the stream function which is defined in the classical form as $u=\partial\psi/\partial y$ and $v=-\partial\psi/\partial x$. Thus, we have

$$\begin{aligned} &u=a\,x^m f'(\eta) \\ &v=-\sqrt{\frac{a\nu(m+1)}{2}}\,x^{(m-1)/2}\left[f(\eta)+\frac{m-1}{m+1}\eta f'(\eta)\right] \end{aligned} \tag{7}$$

where primes denotes differentiation with respect to η. Thus, we define $v_w(x)$ as

$$v_w(x)=-\sqrt{\frac{a\nu(m+1)}{2}}\,x^{(m-1)/2}S \tag{8}$$

where S is the constant mass flux parameter with $S>0$ for suction and $S<0$ for injection. Substituting (6) and (7) into (2) and (3), we obtain the following set of ordinary (similarity) differential equations.

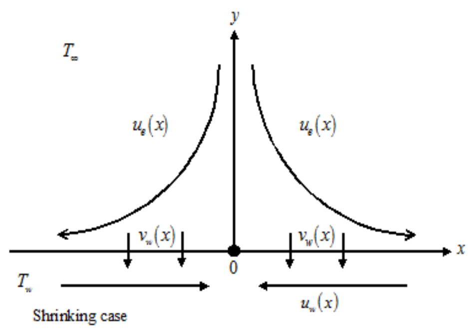

Figure 1. Physical model and coordinate system

$$f'''+f\,f''+\frac{2m}{m+1}\left(1-f'^2\right)=0 \tag{9}$$

$$\frac{1}{\Pr}\theta''+f\,\theta'-\frac{2n}{m+1}f'\theta=0 \tag{10}$$

subject to boundary conditions

$$\begin{aligned} &f(0)=S, \quad f'(0)=\lambda+A\,f''(0), \quad \theta(0)=1+B\theta'(0) \\ &f'(\eta)\to 1, \quad \theta(\eta)\to 0 \quad \text{as} \quad \eta\to\infty \end{aligned} \tag{11}$$

where $\Pr=\nu/\alpha$ is the Prandtl number and $\lambda=c/a$, where $\lambda>0$ for stretching sheet and $\lambda<0$ for shrinking sheet. It is worth mentioning to this end that Eq. (9) is the classical (Falkner-Skan [30]) problem if $\lambda=A=S=0$ where it is more convenient to put $2m/(m+1)=\beta$. Thus, Eq. (9) becomes

$$f''' + f f'' + \beta(1 - f'^2) = 0 \quad (12)$$

subject to the boundary conditions of:

$$f(0)=0, \quad f'(0)=f''(0)$$
$$f'(\eta)\to 1, \quad \text{as} \quad \eta\to\infty \quad (13)$$

There is then a critical value $\beta=\beta_c\approx -0.19884$ and the solution of Eq. (12) is limited in the range of: $\beta\ge\beta_c$.

The quantities of physical interest are the skin friction coefficient C_f and the local Nusselt number Nu_x, which are defined as:

$$C_f=\frac{\tau_w}{\rho u_e^2}, \qquad Nu_x=\frac{x q_w}{k(T_w-T_\infty)} \quad (14)$$

where τ_w is the skin friction or the shear stress along the surface, q_w is the heat flux from the surface of the stretching/shrinking sheet and k is the thermal conductivity, which are given by:

$$\tau_w=\mu\left(\frac{\partial u}{\partial y}\right)_{y=0}, \quad q_w=-k\left(\frac{\partial T}{\partial y}\right)_{y=0} \quad (15)$$

Substituting (6) and (7) into (15) and using (14), we obtain

$$\mathrm{Re}_x^{1/2} C_f=\sqrt{\frac{m+1}{2}}\, f''(0)$$
$$\mathrm{Re}_x^{1/2} Nu_x=-\sqrt{\frac{m+1}{2}}\, \theta'(0) \quad (16)$$

where $\mathrm{Re}_x=u_e(x)x/\nu$ is the local Reynolds number.

3. Results and Discussion

The system of ordinary differential equations (9) and (10) along with the boundary conditions (11) was solved numerically using the shooting method in Maple for $m=1$ (stagnation point flow), $n=0$ (constant surface temperature), $n=1$ (linearly variation of the surface temperature), constant suction parameter $S(>0)$ and shrinking parameter $\lambda(<0)$. In order to simplify the calculations and to conserve space, we consider only the cases $m=1$, $n=0$, $n=1$ and Prandtl number $\mathrm{Pr}=0.71$ of air, throughout the paper. The skin friction coefficient $\mathrm{Re}_x^{1/2} C_f$, the local Nusselt number $\mathrm{Re}_x^{1/2} Nu_x$, the dimensionless velocity $f'(\eta)$ and the dimensionless temperature $\theta(\eta)$ profiles have been obtained and are illustrated in Figures 2 to 15. In order to verify the accuracy of our present method, the values of critical values λ_c for $A=B=m=0$ and several values of positive S (suction) are compared with those reported by Weidman et al. [4] in Table 1. Meanwhile, Table 2 shows the comparison of the values of skin friction coefficient for different values of shrinking parameter when $A=B=S=0$ (impermeable sheet with no slip effects) and $m=1$ (stagnation point flow) with the results obtained by Bhattacharyya et al. [13]. It can be observed that both results are in very good agreement and this gives assurance that our numerical results are accurate and correct.

Table 1. Comparison of the critical values λ_c for different values of S when $A=B=m=0$

S	λ_c **(Present study)**	λ_c **(Weidman et al. [4])**
0.00	-0.3541	-0.3541
0.25	-0.5223	-0.5224
0.50	-0.7201	-0.7200

Table 2. Comparison of the values $\mathrm{Re}_x^{1/2} C_f$ for different values of λ when $A=B=S=0$ and $m=1$

	Present study		**Bhattacharyya et al. [13]**	
λ	**First solution**	**Second solution**	**First solution**	**Second solution**
-0.25	1.40224		1.40224	
-0.50	1.49567		1.49567	
-0.615	1.50724		1.50724	
-0.75	1.48930		1.48930	
-1.00	1.32882	0	1.32882	0
-1.15	1.08223	0.11670	1.08223	0.11667
-1.20	0.93247	0.23365	0.93247	0.23365
-1.2465	0.58428	0.55429	0.58429	0.55429

Figures 2 and 3 show the variations of the skin friction coefficient $\mathrm{Re}_x^{1/2} C_f$ and the local Nusselt number $\mathrm{Re}_x^{1/2} Nu_x$, respectively, with shrinking parameter λ for different values of the suction parameter S. These two figures indicate that dual solutions (upper and lower branch solutions) for Eqs. (9) and (10) with the boundary conditions (11) exist in the range $\lambda_c<\lambda\le 0$ (shrinking sheet), where $\lambda_c(<0)$ is the critical value of λ for which solutions of the boundary value problem (9 - 11) exist. Unique solution exists for $\lambda=\lambda_c$ and no solution exists for $\lambda<\lambda_c<0$, where the boundary layer separates from the surface of the sheet and the solutions based upon the boundary layer approximations are not possible for each value of S. In this case, the full Navier-Stokes and energy equations have to be solved. It is seen in Figures 2 and 3 that both $\mathrm{Re}_x^{1/2} C_f$ and $\mathrm{Re}_x^{1/2} Nu_x$ increase with the increase of the suction parameter S for an upper branch solution. However, it is found that $\mathrm{Re}_x^{1/2} C_f$ decreases for the lower branch solution, but $\mathrm{Re}_x^{1/2} Nu_x$

increases as the suction parameter S increases. Figures 2 and 3 also show that the suction parameter S delays the boundary layer separation.

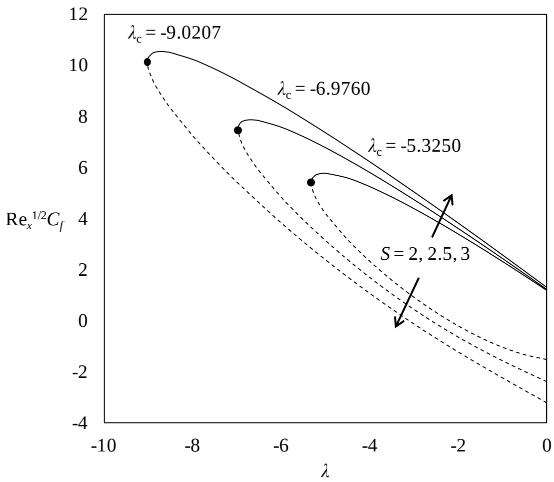

Figure 2. Variation of $\mathrm{Re}_x^{1/2} C_f$ with λ for several values of S when $A = B = 0.5$, $m = 1$

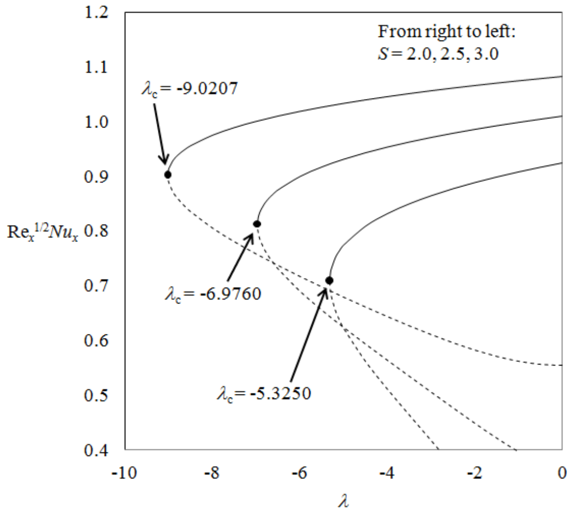

Figure 3. Variation of $\mathrm{Re}_x^{1/2} Nu_x$ with λ for several values of S when $A = B = 0.5$, $S = 2.5$ $m = 1$, $n = 0$ and $\Pr = 0.71$

Figures 4 to 8 depict the variations of the skin friction coefficient $\mathrm{Re}_x^{1/2} C_f$ and the local Nusselt number $\mathrm{Re}_x^{1/2} Nu_x$ with shrinking parameter λ for different values of the constant velocity slip parameter A and constant temperature slip parameter B. Here, in Figures 7 and 8, we have investigated the effects of both parameters A and B at a constant surface temperature ($n = 0$). From Figures 4, 5 and 7, we found that the values of shrinking parameter $|\lambda|$ for which the solution exist increases as the parameter A increases. Hence, the velocity slip parameter A delays the boundary layer separation. However, based on different observations examined in Figures 6 and 8 the critical value λ_c is the same ($\lambda_c = -6.9760$) for any value of the considered parameter $B (B = 0, 0.5, 1, 3)$. Therefore, parameter B does not affect the boundary layer separation. It is, however, worth mentioning that parameter B does not affect the variation of $\mathrm{Re}_x^{1/2} C_f$ due to the decoupled Equations of (9) and (10).

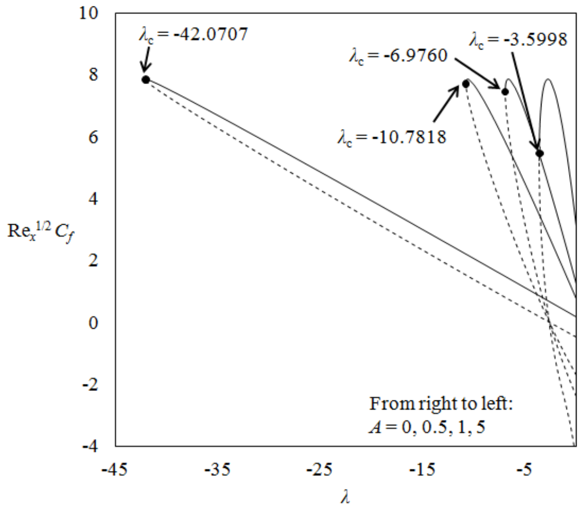

Figure 4. Variation of $\mathrm{Re}_x^{1/2} C_f$ with λ for several values of A when $B = 0.5$, $S = 2.5$ and $m = 1$

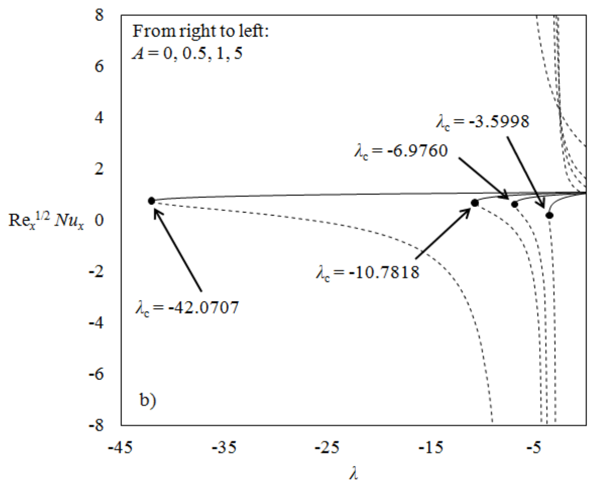

Figure 5. Variation of $\mathrm{Re}_x^{1/2} Nu_x$ with λ for several values of A when $B = 0.5$, $S = 2.5$, $m = n = 1$ and $\Pr = 0.71$

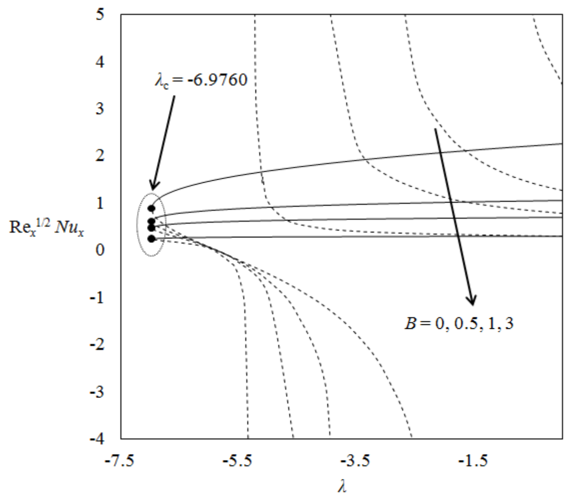

Figure 6. Variation of $\mathrm{Re}_x^{1/2}\,Nu_x$ with λ for several values of B when $A=0.5$, $S=2.5$, $m=n=1$ and $\mathrm{Pr}=0.71$

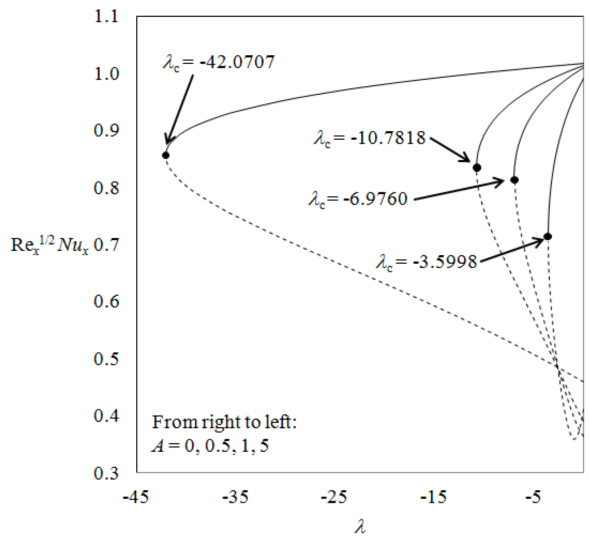

Figure 7. Variation of $\mathrm{Re}_x^{1/2}\,Nu_x$ with λ for several values of A when $B=0.5$, $S=2.5$ $m=1$, $n=0$ and $\mathrm{Pr}=0.71$

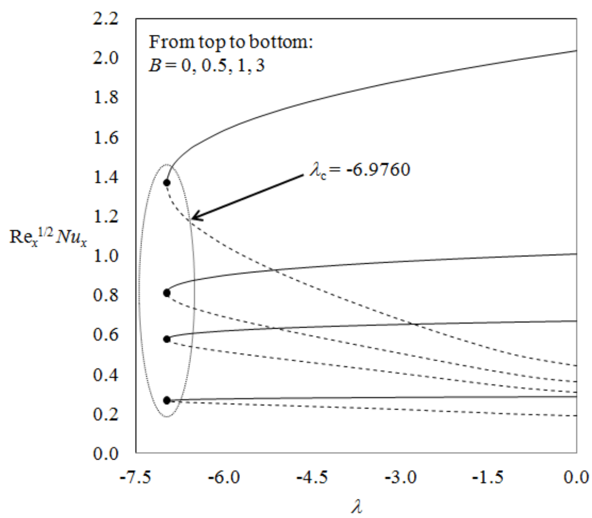

Figure 8. Variation of $\mathrm{Re}_x^{1/2}\,Nu_x$ with λ for several values of B when $A=0.5$, $S=2.5$ $m=1$, $n=0$ and $\mathrm{Pr}=0.71$

The velocity and temperature profiles for several values of suction parameter S are depicted in Figures 9 and 10. Meanwhile, the velocity and temperature profiles for several value of positive constant velocity slip parameter A and positive constant temperature slip parameter B are shown in Figures 11 to 15. However, Figures 14 and 15 display the temperature profile when $n=0$ (constant surface temperature). It is obvious that the upper branch solution shows the thinner boundary layer thickness compared with the lower branch solution. Figures 9, 10 and 15 show that the boundary layer thicknesses decrease (upper and lower branches) with the increasing value of suction parameter S (Figures 9 and 10) and positive constant temperature slip parameter B (Figure 15). This finding supports the fact that a suction process on a laminar boundary layer reduces the thickness of the boundary layer and makes the boundary layer fuller near the wall. It can be seen that in Figures 11 and 14, the velocity and thermal boundary layer thicknesses decrease for the upper branch solutions and increase for the lower branch solutions with the increase of positive constant velocity slip parameter A. It can also be illustrated that by Figures 12 and 13, for both upper and lower branch solutions, the thermal boundary layer thickness increases as positive constant temperature slip parameter B increases. It is also shown in Figures 9 to 15 that the boundary layer thicknesses are much larger for the lower branch solutions than for the upper branch solutions. These profiles support the existence of the dual nature of the solutions presented in Figures 2 to 8. They also satisfy the far field boundary conditions (11) asymptotically.

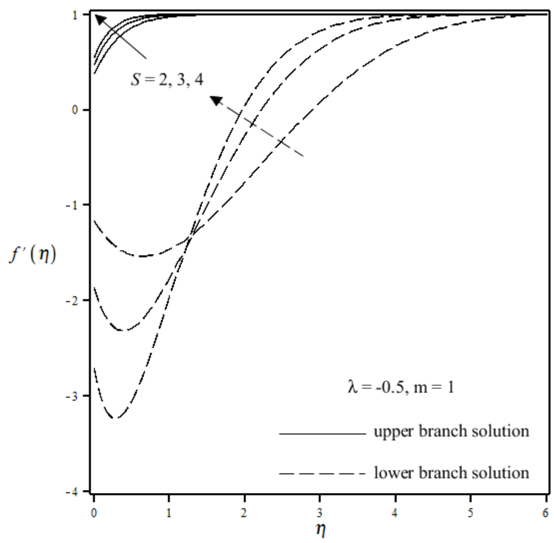

Figure 9. Velocity profile $f'(\eta)$ for several values of S when $\lambda=-0.5$, $A=B=0.5$ and $m=1$

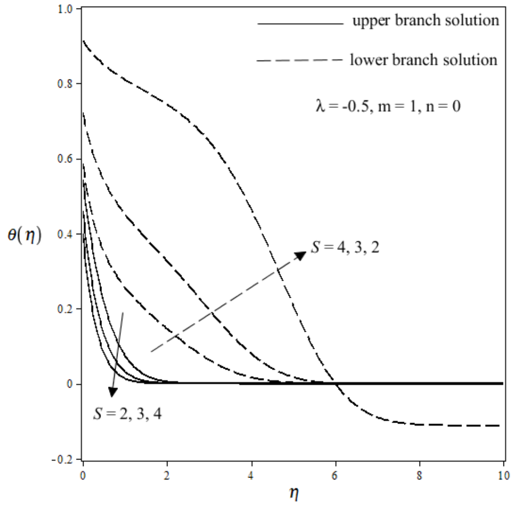

Figure 10. Temperature profile $\theta(\eta)$ for several values of S when $\lambda = -0.5$, $A = B = 0.5$, $m = 1$, $n = 0$ and $\mathrm{Pr} = 0.71$

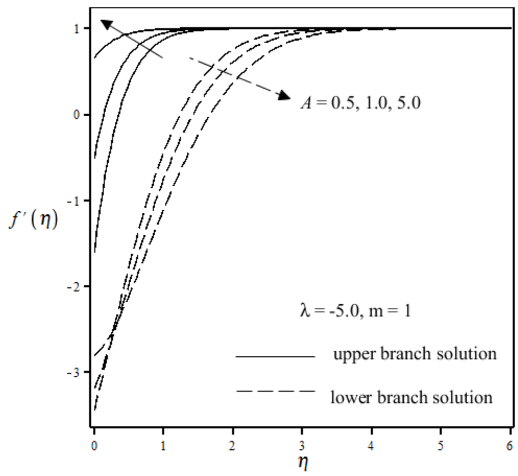

Figure 11. Velocity profile $f'(\eta)$ for several values of A when $\lambda = -5.0$, $B = 0.5$, $S = 2.5$ and $m = 1$

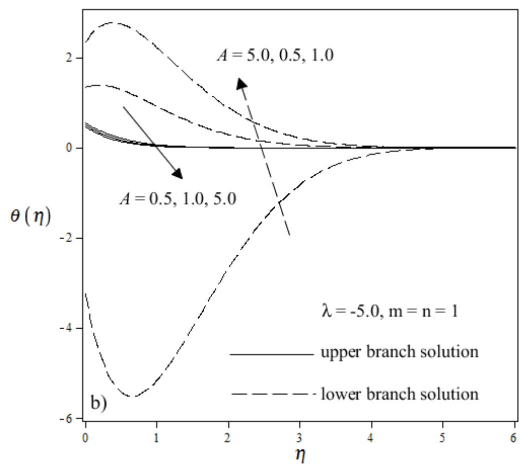

Figure 12. Temperature profile $\theta(\eta)$ for several values of A when $\lambda = -5.0$, $B = 0.5$, $S = 2.5$, $m = n = 1$ and $\mathrm{Pr} = 0.71$

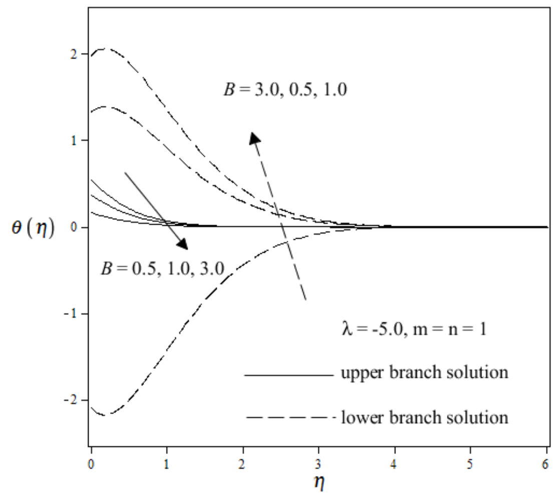

Figure 13. Temperature profile $\theta(\eta)$ for several values of B when $\lambda = -5.0$ $A = 0.5$, $S = 2.5$, $m = n = 1$ and $\mathrm{Pr} = 0.71$

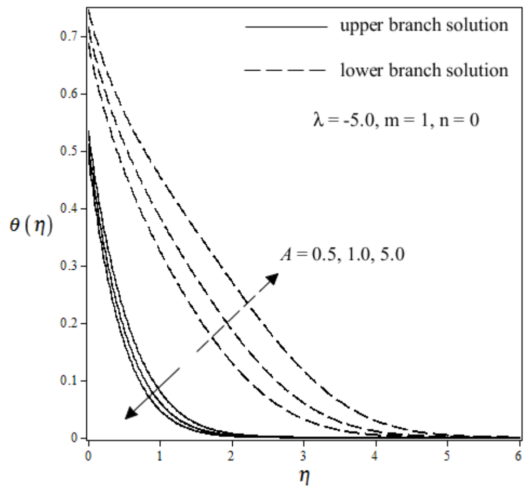

Figure 14. Temperature profile $\theta(\eta)$ for several values of A when $\lambda = -5.0$, $B = 0.5$, $S = 2.5$, $m = 1$, $n = 0$ and $\mathrm{Pr} = 0.71$

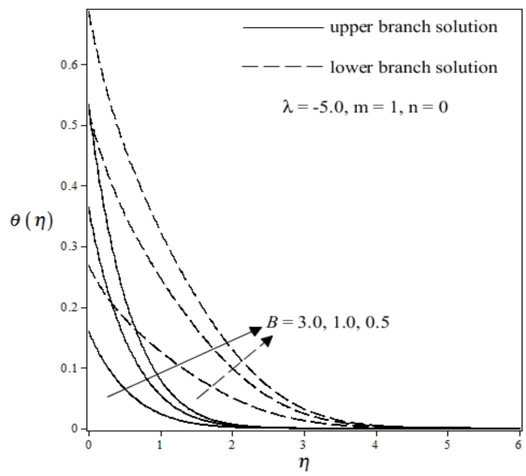

Figure 15. Temperature profile $\theta(\eta)$ for several values of B when $\lambda = -5.0$, $A = 0.5$, $S = 2.5$, $m = 1$, $n = 0$ and $\mathrm{Pr} = 0.71$

4. Conclusion

The problem of stagnation point flow and heat transfer over a permeable shrinking sheet with slip effects has been solved numerically to exhibit the effects of the suction parameter on the velocity and temperature distributions. From this study, we can conclude that:

- dual solutions exist (first and second solutions) for a certain range of the shrinking parameter,
- the suction parameter increases the skin friction coefficient and the local Nusselt number for the upper branch solution, while decreases the skin friction coefficient and increases the local Nusselt number for the lower branch solutions,
- the suction process reduces the boundary layer thickness and delays the boundary layer separation,
- the velocity slip delays the boundary layer separation. Meanwhile, temperature slip does not affect the boundary layer separation.

Acknowledgements

The second and third authors wish to thank the Department of Higher Education, Ministry of Education Malaysia for financial support received under the Fundamental Research Grant Scheme (Project Code: 203/PJJAUH/6711293). The support provided by the Universiti Sains Malaysia is also acknowledged. The authors also wish to express their thanks to the very competent Reviewers for the very good comments and suggestions.

References

[1] T. C. Chiam, "Stagnation-point flow towards a stretching plate," *J. Phys. Soc. Japan*, vol. 63, pp. 2443–2444, 1994.

[2] T. R. Mahapatra, A. S. Gupta, "Magnetohydrodynamic stagnation-point flow towards a stretching," *Acta Mech.*, vol. 152, no. 1, pp. 191–196, 2001.

[3] T. R. Mahapatra, A. S. Gupta, "Heat transfer in stagnation-point flow towards a stretching sheet," *Heat Mass Transfer*, vol. 38, no. 6, pp. 517–521, 2002.

[4] P. D. Weidman, A. M. J. Davis, D. G. Kubitschek, "The effects of transpiration on self-similar boundary layer flow over moving surfaces," *Int. J. Eng. Sci.*, vol. 44, no. 11-12, pp. 730–737, 2006.

[5] C. Y. Wang, "Flow due to a stretching boundary with partial slip – an exact solution of the Navier-Stokes equations," *Chem. Eng. Sci.*, vol. 57, no. 17, pp. 3745–3747, 2002.

[6] A. V. Roşca, I. Pop, "Flow and heat transfer over a vertical permeable stretching/shrinking sheet with a second order slip," *Int. J. of Heat and Mass Transfer*, vol. 60, pp. 355–364, 2013.

[7] F. Aman, A. Ishak, I. Pop, "Magnetohydrodynamic stagnation-point flow towards a stretching/shrinking sheet with slip effects," *Int. Commun. in Heat and Mass Transfer*, vol. 47, pp. 68–72, 2013.

[8] A. M. Rohni, S. Ahmad, A. I. Md. Ismail, I. Pop, "Boundary layer flow and heat transfer over an exponentially shrinking vertical sheet with suction," *Int. J. of Thermal Sciences*, vol. 64, pp. 264–272, 2013.

[9] A. M. Rohni, S. Ahmad, I. Pop, "Flow and heat transfer at a stagnation-point over an exponentially shrinking vertical sheet with suction," *Int. J. of Thermal Sciences*, vol. 75, pp. 164–170, 2014.

[10] S. A. Al-Sanea, "Mixed convection heat transfer along a continuously moving heated vertical plate with suction or injection," *Int. J. Heat Mass Transfer*, vol. 47, no. 6-7, pp. 1445–1465, 2004.

[11] E. M. Sparrow, J. P. Abraham, "Universal solutions for the stream-wise variation of the temperature of a moving sheet in the presence of a moving fluid," *Int. J. Heat Mass Transfer*, vol. 48, no. 15, pp. 3047–3056, 2005.

[12] K. Bhattacharyya, "Dual solutions in unsteady stagnation-point flow over a shrinking sheet," *Chin. Phys. Lett.*, vol. 28, no. 8, 08472, 2011.

[13] K. Bhattacharyya, S. Mukhopadhyay, G. C. Layek, "Slip effects on boundary layer stagnation-point flow and heat transfer towards a shrinking sheet," *Int. J. Heat Mass Transfer*, vol. 54, no. 1-3, pp. 308–313, 2011.

[14] K. Bhattacharyya, I. Pop, "MHD boundary layer flow due to an exponentially shrinking sheet," *Magnetohydrodynamics*, vol. 47, pp. 337–344, 2011.

[15] K. Bhattacharyya, G. C. Layek, "Effects of suction/blowing on steady boundary layer stagnation-point flow and heat transfer towards a shrinking sheet with thermal radiation," *Int. J. Heat Mass Transfer*, vol. 54, no. 1-3, pp. 302–307, 2011.

[16] K. Bhattacharyya, K. Vajravelu, "Stagnation-point flow and heat transfer over an exponentially shrinking sheet," *Commun. Nonlinear Sci. Numer. Simulat.*, vol. 17, no. 7, pp. 2728–2734, 2012.

[17] K. Vajravelu, "Viscous flow over a nonlinearly stretching sheet," *App. Math. And Comp.*, vol. 124, no. 3, pp. 281–288, 2001.

[18] R. Nazar, N. Amin, D. Filip, I. Pop, "Unsteady boundary layer flow in the region of the stagnation point on a stretching sheet," *Int. J. of Eng. Sci.* , vol. 42, no. 11-12, pp. 1241–1253, 2004.

[19] S. Nadeem, A. Hussain, M. Khan, "HAM solutions for boundary layer flow in the region of the stagnation point towards a stretching sheet," *Commun. Nonlinear Sci. Numer. Simulat.*, vol. 15, no. 3, pp. 475–481, 2010.

[20] A. M. Rohni, S. Ahmad, I. Pop, "Note on Cortell's non-linearly stretching permeable sheet," *Int. J. Heat Mass Transfer*, vol. 55, no. 21-22, pp. 5846–5852, 2012.

[21] K. Bhattacharyya, "Heat transfer analysis in unsteady boundary layer stagnation-point flow towards a shrinking/stretching sheet," *Ain Shams Eng. J.*, vol. 4, no. 2, pp. 259–264, 2013.

[22] S. Yao, T. Fang, Y. Zhong, "Heat transfer of a generalized stretching/shrinking wall problem with convective boundary conditions," *Commun. Nonlinear Sci. Numer. Simulat.*, vol. 16, no. 2, pp. 752–760, 2011.

[23] Y. Seini, O. D. Makinde, "Boundary layer flow near stagnation-points on a vertical surface with slip in the presence of transverse magnetic field," *Int. J. Numer.*

Methods Heat & Fluid Flow, vol. 24, no. 3, pp. 643–653, 2014.

[24] O. D. Makinde, "Computational modelling of nanofluids flow over a convectively heated unsteady stretching sheet," *Current Nanoscience*, vol. 9, no. 5, pp. 673–678, 2013.

[25] S. Shateyi, O. D. Makinde, "Hydromagnetic stagnation-point flow towards a radially stretching convectively heated disk," *Mathem. Problems in Engng*., vol. 2013, Article ID. 616947, 8 pages, 2013.

[26] O. D. Makinde, W. A. Khan, Z. H. Khan, "Buoyancy effects on MHD stagnation point flow and heat transfer of a nanofluid past a convectively heated stretching/shrinking sheet," *Int. J. Heat Mass Transfer*, vol. 62, pp. 526–533, 2013.

[27] A. M. Olanrewaju, O. D. Makinde, "On boundary layer stagnation point flow of a nanofluid over a permeable flat surface with Newtonian heating," *Chemical Engng. Comm*., vol. 200, no. 6, pp. 836–852, 2013.

[28] N. C. Roşca, I. Pop, "Mixed convection stagnation point flow past a vertical flat plate with a second order slip: heat flux case," *Int. J. Heat Mass Transfer*, vol. 65, pp. 102–109, 2013.

[29] A. V. Roşca, N. C. Roşca, I. Pop, "Axisymmetric stagnation point flow and heat transfer towards a permeable moving flat plate with surface slip condition," *Appl. Math. Comp*., vol. 233, pp. 139–151, 2014.

[30] V. M. Falkner, S. W. Skan, "Some approximate solutions of the boundary layer equations," *Phil. Mag*., vol. 12, pp. 865–896, 1931.